Journal of Mechanical Engineering Research and Developments
ISSN: 1024-1752
CODEN: JERDFO
Vol. 43, No. 6, pp. 184-196
Published Year 2020

Numerical Study of Lid Driven Mixed Convection in Inclined Wavy Cavity

Mohammed Mousa Al-azzawi[†], Ayad K. Hassan[‡], Humam Kareem Jalghaf[†‡], Laith Jaafer Habeeb[‡‡]

[†]Department of Refrigeration and Air Conditioning, Al-Rafidain University Collage, Baghdad, Iraq
[‡]University of Technology, Materials Engineering Department, Baghdad, Iraq
[†‡]Mechanical Engineering Department University of Technology, Baghdad, Iraq
[‡‡]Training and Workshop Centre, University of Technology, Baghdad, Iraq
E-mail: 20021@uotechnology.edu.iq

ABSTRACT: The present paper deals with a numerical study of the hydrodynamic and thermal characteristics resulted from mixed convection in four shapes of wavy cavity at different angles of inclination. The top horizontal cooled wall moving as lid-driven is kept at constant temperature T_C and the bottom hot wall is kept at constant temperature T_h. The stream function – vorticity approach is being used to answer differential equations and the translation of the directions is achieved by transforming the wavy form obsessed by a rectangle control volume. Validation was performed by comparison t He discussed research with prior findings and noticed that he was in outstanding agreement. The range of dimensionless parameters (Reynolds and Richardson numbers) were $27 \leq Re \leq 845$ and $0:01 \leq Ri \leq 10$ with constant Grashof number Gr=7142. The angles of inclination $\varphi = 0^o$, 45^o, and 90^o. Reports were described in terms of rationales, isotherms and overall Nusselt numbers. It was found that the average There is no effect on the heat transfer cycle for angle of inclination. Nusselt number increases with the growth Richardson number. The heat transfer coefficient enhances in a wavy cavity as the amplitude and number of corrugations increase.

KEYWORDS: mixed convection, cavity, driven-lid.

INTRODUCTION

Fundamental natures and relevance of lid-driven flows in cavities are relevant to many heat transfer engineering presentations. Examples of these applications can be related to the oil extraction in grooved wet clutches, solar concentrator and thermal efficiency improvement of heat exchangers [1]. Other instances include electronic cooling equipment, food-drying, heat pumps and power plants [2]. For the related problems, a wavy cavity with driven-lid is used for analyzing the heat and fluid transport characteristics. A moving top wall controls the flow, and heat transfer occurs because of a temperature difference between the top and bottom walls. In recent years, several authors researched normal, induced, and mixed convection in a cavity under a broad range of thermal boundary conditions in different cavity geometries.

Chen and Cheng (2004), [1] studied Experimentally and numerically the effects of lid movement represented by Reynolds number and buoyancy represented by Grashof number on fluid flow and thermal fields For combined natural convection around an arc-shaped chamber guided by the cap. Fluid flow, relative roughness, and numbers of Nusselt were studied in a wide range of numbers Grashof and Reynolds. Hakan (2006), [2] analyzed the combined convection in a porous lid driven hot cavity with moving the upper cold wall at constant velocity from the left to the right. The author revealed that the best heat transfer occurs if the heating is placed on the left vertical wall. Sharif (2007), [3] used water as a working fluid to study the mixed convection heat transfer inside inclined rectangular driven cavity with moving top hot lid -driven. He concluded that the heat transfer rates enhance as the cavity inclination angle

moves from vertical to horizontal position, and the forced convection is the dominating factor in the heat transfer process. Chaves et al. (2008), [4] studied the combined effects of lid-driven movement and buoyancy forces in a semi porous open cavity. The results show that the maximum heat transfer rates occur at the bottom wall. Wang (2009), [5] studied the mixed convection heat transfer inside rectangular cavity contains a porous Darcy–Brinkman medium with lid-driven. He concluded that the strong effect of eddies reduces due to presence of porous medium especially for deep cavity. Stephen and Kambiz (2010), [6] studied the combined buoyancy induced flow and vibration on the left vertical wall of porous medium cavity. They concluded that the vibrational effects on the heat transfer process becomes strong at high values of Darcy and Reynolds numbers. On the other side, lower Darcy number and higher modified Rayleigh numbers have caused strong buoyancy effects. Mohd et. al. (2010), [7] concluded that the porosity has great effect on the boundary layer velocity and gives a strong vortex inside a lid-driven square cavity filled with porous media. Nemati et al. (2010), [8] Lattice Boltzmann Process used to analyze mixed convection flows using nanofluids in a cavity guided by the cap. The cavity fluid is a water dependent nanofluid containing nanoparticles Cu, Cuo, or Al2O3. The effects on hydrodynamic and thermal properties of the Reynolds number and solid volume fraction for specific nanofluids are studied. The findings show that the effects of the solid volume fraction for Al2O3, Cuo and Cu grow stronger sequentially. Additionally, the increase in the number of Reynolds contributes to a decrease in the effect of the solid concentration.Rahman et al. (2011), [9] used Galerkin finite element method to study numerically the behavior of nanofluid in an inclined lid-driven triangular enclosure. Copper-water nanofluids with Prandtl size, Pr = 6.2 and solid particle size values were 0%, 4%, 8 % and 10%. We concluded that at the three convective systems, the solid volume fraction greatly affected the fluid flow and heat transfer inside the enclosure.Gazy et. al. (2012), [10] Study of the effect of the particles size of the drying chamber of spherical particles on the heat transfer of the integrated circular tube.They concluded that using the porous media with large particles around the heated cylinder improves the heat transfer process. Khaled et al. (2012) [11], examined the effects of the moving lid-direction on the MHD mixed convection in a cavity. The bottom wall was heated linearly while the vertical walls were. The results show that the case of mixed convection is better than the case of forced convection for giving more effective flow in the direction of lid and more heat transfer rate. Gazy and Mark (2013), [12] found that the heat transfer rate from the cylinder placed in a porous medium filled channel is better than that in empty channel. Abdelraheem and Sameh (2014), [13] investigated the natural and mixed convective heat transfer in a saturated cavity. It was concluded that the heat transfer rate and the flow regime are affected strongly by permeability ratio and angle of inclination. Chen and Chung (2015), [14] studied the fluid behavior and thermal fields In a compelled triangular chamber, which is confined to a moving lid. They studied the influence of the angle of inclination, the number of Reynolds, and Grashof number under wide ranges of these parameters on isotherms and streamlines. They showed that here are three types of flow regime in an inclined triangular hollow: buoyancy region, inertia-region, and mixed convection region. Burgos et al. (2016), [15] studied steady and unsteady two-dimensional mixed convection in a channel with an open square cavity and a heated bottom wall. It was shown that for Richardson number less than 0.1, The effect of the buoyancy on all values of the Reynolds number considered was negligible. This effect increases for Ri = 1 and 10. Ilhem and Rachid (2017), [16] studied using finite volume method the laminar flow and heat transfer in a lid-driven square cavity filled with a nanofluid. The two vertical walls were heated simultaneously at a constant heat flux. The moving wall and the underside wall of the chamber were kept constant cold temperatures. The position of the heat source has been identified as having a strong influence on fluid and thermal behavior patterns. Ali et al. (201-), [17] studied the two-dimensional aiding and opposing flow and heat transfer in trapezoidal lid-driven cavity filled with four types of nanofluids. They found that SiO_2-water and the aiding flow give the higher heat transfer rate than other nanofluids and aiding flow. Kefayati and Tang (2018), [18] studied the effect of magnetic field on the heat transfer and viscoelastic fluid flow in lid-driven enclosure with differentially heated sidewalls. Results show that, the middling Nusselt number gradually and the unyielded parts increase significantly as Hartmann number increases.

The present work comprises a numerical study of the hydrodynamic and thermal characteristics resulted from mixed convection in different four shapes of inclined wavy cavity with a top cooled wall moving as

lid-driven. The bottom hot wall is kept at constant temperature T_h. The working fluid is air with Pr=0.71. The range of Reynolds number, Richardson number, and angle of inclination were: $27 \leq Re \leq 845$, $0.01 \leq Ri \leq 10$, $0^o \leq \varphi \leq 90^o$; respectively.

MATHEMATICAL MODEL

Find tending wavy hollow subject to differential of flowing lid & temperature, as seen in Figure 1a. The wavy hollow is curved from the parallel to the horizontal. The lid transfers continuously at a constant velocity (u0) through the hollow lengthways the highest lateral of the triangle. The moving lid is maintained at a constant lower temperature (Tl), while the bottom wall is retained at a steady higher temperature (T_h). While the other vertical wavy walls are adiabatic. The angles of inclination are 0^o, 45^o, and 90^o, individually. [18] suggested the mathematical definition for mixed heat transfer in an inclined arc-shaped cavity. The mathematical model of this work has been employed and expanded in an inclined wavy cavity to examine the flow pattern and heat transfer characteristics, and is limited functionality following.

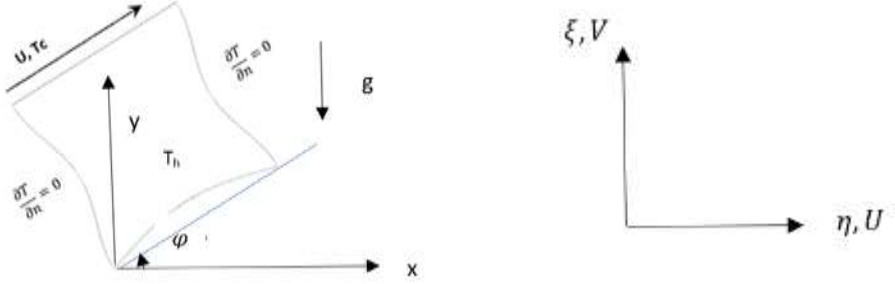

a. Physical domain

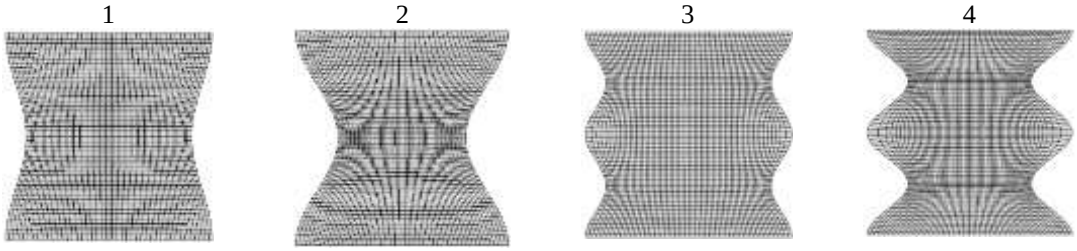

N=1, λ =0.1 N=1, λ =0.2 N=2, λ =0.1 N=2, λ =0.2

b. Computational domain

Figure 1. Diagram description of an inclination triangular cavity due to a flowing lid and differential temperature: (a) fleshly environment, and (b) computer to find.

The numerical function refers to the surface of a corrugated wall of a square cavity is given in table 1

Table 1. mathematical function of the corrugation annuls surfaces.

$N =$ number of corrugations
$\lambda =$ amplitude.
φ =angle of inclination (deg)
For symmetry simulationφchanged from 0 to $\frac{\pi}{2}$

$$x = R + \lambda \, sin \, sin \left(\frac{N.\varphi.\frac{\pi}{180}}{N} \right) . (cos(\varphi.\frac{\pi}{180}))$$

$$y = R + \lambda \, sin \, sin \left(\frac{N.\varphi.\frac{\pi}{180}}{N} \right) . (sin(\varphi.\frac{\pi}{180}))$$

Governing Equations

The viscous incompressible two-dimensional laminar air flow in the cavity is governed by continuity, momentum, and energy equations. The fluid properties are assumed to be constant except the density variation in the buoyant force according to Boussinesq approximation. The stream function – vorticity approach is being used to solution the continuity equation and vectors are transformed to map the wavy shape into a rectangular test section, as seen in Figure 1b. In Equations (1–3), the governing equations are given using dimensional vorticity (Ω), stream function (Ψ), and dimensional temperature (θ), which are centered into body-fitted wavy organize (ξ, η). Such equations contain together the concepts of inertial force and floating force

$$c_1\frac{\partial^2\Psi}{\partial\eta^2}-2c_2\frac{\partial^2\Psi}{\partial\xi\partial\eta}+c_3\frac{\partial^2\Psi}{\partial\xi^2}=-J^2\Omega \tag{1}$$

$$\frac{\partial\Omega}{\partial\xi}\frac{\partial\Psi}{\partial\eta}-\frac{\partial\Omega}{\partial\eta}\frac{\partial\Psi}{\partial\xi}=\frac{1}{JRe}\left(c_1\frac{\partial^2\Psi}{\partial\eta^2}-2c_2\frac{\partial^2\Psi}{\partial\xi\partial\eta}+c_3\frac{\partial^2\Psi}{\partial\xi^2}\right)+\frac{Gr}{Re^2}\left\{cos\varphi\left(\frac{\partial Y}{\partial\eta}\frac{\partial\theta}{\partial\xi}-\frac{\partial Y}{\partial\xi}\frac{\partial\theta}{\partial\eta}\right)-sin\varphi\left(\frac{\partial X}{\partial\xi}\frac{\partial\theta}{\partial\eta}-\frac{\partial X}{\partial\eta}\frac{\partial\theta}{\partial\xi}\right)\right\} \tag{2}$$

$$\frac{\partial\theta}{\partial\xi}\frac{\partial\Psi}{\partial\eta}-\frac{\partial\theta}{\partial\eta}\frac{\partial\Psi}{\partial\xi}=\frac{1}{JRePr}\left(c_1\frac{\partial^2\theta}{\partial\eta^2}-2c_2\frac{\partial^2\theta}{\partial\xi\partial\eta}+c_3\frac{\partial^2\theta}{\partial\xi^2}\right) \tag{3}$$

We can express the equations. (1–3) In Jacobian terms, of the rectangular coordinate transformation (X,Y) to the wavy manages (ξ,η) as shown in Eq. (4); and is expressed in Eq. (5). Here in education, Prandtl number is usual to 0.71 for air.

$$\Omega=\omega L/u_o\,;\quad \Psi=\phi/u_oL\,;\ \theta=(T-T_l)/(T_h-T_l) \tag{4}$$

$$J=\frac{\partial Y}{\partial\xi}\frac{\partial X}{\partial\eta}-\frac{\partial Y}{\partial\eta}\frac{\partial X}{\partial\xi} \tag{5}$$

$$c_1=\left(\frac{\partial X}{\partial\eta}\right)^2+\left(\frac{\partial Y}{\partial\eta}\right)^2\ ;\ c_2=\frac{\partial X}{\partial\xi}\frac{\partial X}{\partial\eta}+\frac{\partial Y}{\partial\eta}\frac{\partial Y}{\partial\xi}\ ;\ c_1=\left(\frac{\partial X}{\partial\xi}\right)^2+\left(\frac{\partial Y}{\partial\xi}\right)^2 \tag{6}$$

$$X=x/L;\ \ Y=y/L\,;\ U=u/u_o;\ \ V=v/u_o \tag{7}$$

$$Gr=g\beta(T_h-T_l)L^3/\vartheta^2\,;\qquad Re=u_oL/\vartheta\ ;\qquad Pr=\vartheta/\alpha \tag{8}$$

The condensed stream function and vortices, as expressed, are connected to Undimensional velocities in Eqs. (9) and (10):

$$\Omega=\frac{1}{J}\left[\left(\frac{\partial V}{\partial\xi}\frac{\partial Y}{\partial\eta}-\frac{\partial V}{\partial\eta}\frac{\partial Y}{\partial\xi}\right)+\frac{\partial U}{\partial\xi}\frac{\partial X}{\partial\eta}-\frac{\partial U}{\partial\eta}\frac{\partial X}{\partial\xi}\right] \tag{9}$$

$$U=\frac{1}{J}\left(-\frac{\partial\Psi}{\partial\xi}\frac{\partial X}{\partial\eta}+\frac{\partial\Psi}{\partial\eta}\frac{\partial X}{\partial\xi}\right);\qquad V=\frac{1}{J}\left(-\frac{\partial\Psi}{\partial\xi}\frac{\partial Y}{\partial\eta}+\frac{\partial\Psi}{\partial\eta}\frac{\partial Y}{\partial\xi}\right) \tag{10}$$

Boundary Conditions

The boundary environments on the cold touching lid and the hot wall are given in Eqs. (11) and (12), respectively:

$$U=1;\quad V=0;\quad \Psi=0;\quad \theta=0;\quad \Omega=-\frac{1}{J}\left(\frac{\partial U}{\partial\eta}\frac{\partial X}{\partial\xi}\right) \tag{11}$$

$$U = 0; \quad V = 0; \quad \Psi = 0; \quad \theta = 1; \quad \Omega = -\frac{1}{J}\left(\frac{\partial V}{\partial \eta}\frac{\partial Y}{\partial \xi} + \frac{\partial U}{\partial \eta}\frac{\partial X}{\partial \xi}\right) \quad (12)$$

Solution Procedure

The finite-volume approach discretizes the equations (1-3), and the boundary conditions (11 and 12). Calculation of Generation of grids is centered on the curvilinear interface frame(ξ, η). The transition of coordinates functions (i.e., $\xi = \zeta(X, Y)$ and $\eta = \eta(X, Y)$) were planned by Thompson et al. [19] and accepted by Chen, et al. [20]. The finite-volume terms for Ψ, Ω and θ may be solved together by means of the restatement process. The dominant way of distinction is extended to the Discretion process. The transition does work $\xi = \zeta(X, Y)$ and $\eta = \eta(X, Y)$ Are extracted differently by executing the complex two Poisson elliptic equations, as provided in Eq. (13):

$$\frac{\partial^2 \xi}{\partial X^2} + \frac{\partial^2 \xi}{\partial Y^2} = P(X, Y) \qquad (13\ a)$$

$$\frac{\partial^2 \eta}{\partial X^2} + \frac{\partial^2 \eta}{\partial Y^2} = Q(X, Y) \qquad (13\ b)$$

Anywhere P and Q are 2 uninformed functions defined for local grid density adjustment. To increasing the statistical accuracy, the successive over-relaxation approach was adopted. For stream function, vorticity and energy equations the adopted relaxation factors are 0.1, 1.5, and 1.0, respectively. Cheng and Chen [21, 22] provide thorough report for this answer method.

System Characteristics

The overall heat transfer coefficient h x (X) on the traveling lid is expressed in Eqs as well as the local Nusselt number Nuw x on the moving lid. (14) and (15), i.e.:

$$h_x(X) = \frac{\kappa}{(T_h - T_l)}\frac{\partial T}{\partial n}\Big|_{moving\ lid} \qquad (14)$$

$$Nu_x = h_x(X)L/\kappa \qquad (15)$$

While n is the usual external coordinate for the traveling lid or where ÿ is the thermal conductivity of the fluid. The total heat transfer coefficient h aveand the total number Nusselt$Nu_{\ ave}$ may be calculated by Eq. (16 and 17):

$$h_{ave} = \int_0^1 h_x\,(X)\,dX/L \qquad (16)$$

$$Nu_{ave} = h_{ave}L/\kappa \qquad (17)$$

The regional resistance factor f x on the moveable cloak was correlated with the central shear stressτ_x is calculated as follows:

$$f_x = \frac{\tau_x}{\rho u_o^2} = \frac{\mu}{\rho u_o^2}\frac{\partial u}{\partial y}\Big|_{moving\ lid} = \frac{1}{JRe}\frac{\partial X}{\partial \xi}\frac{\partial U}{\partial \eta}\Big|_{moving\ lid} \qquad (18)$$

Where μ is fluid dynamic viscosity.

For the grid generation, the suitable choice of the used technique to transmission the physical field addicted to computational field has a big effect on the solution. The orthogonally of the generated grids system can be improved by carefully setting the boundary conditions. **Figure 1-b** reveals the symbol cases of curvilinear grid system applied in this study.

The temporal discretization method employed for the current study is a two- and three- step time-splitting scheme for the energy and momentum equations, correspondingly. Figure 2 shows the values of average Nusselt number for different grid numbers and four types of wavy cavity types at Ri=10, $\varphi = 0^o$. As shown in this figure that the increasing of grid numbers greater than 60 gives nearly identical results. So, the grid number of domains was chosen as 60.

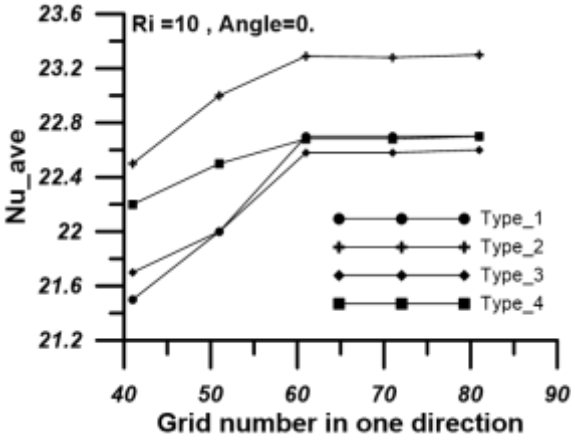

Figure 2. Average Nusselt number versus grid number in one direction for four types of wavy cavity, at Ri=10, $\varphi = 0^o$.

Code validation

The numerical solution methodology used in our code was validated by comparing its results for streamlines and isotherms with the analytical results reported by Chen and Cheng [20] as shown in Fig. 3 for the problem of mixed convection with periodic flow pattern and heat transfer in a lid-driven arc-shape cavity. It can be seen that the numerical model is in a good agreement with work [20] for Re=1000, $Gr=10^6$ and 10^7.

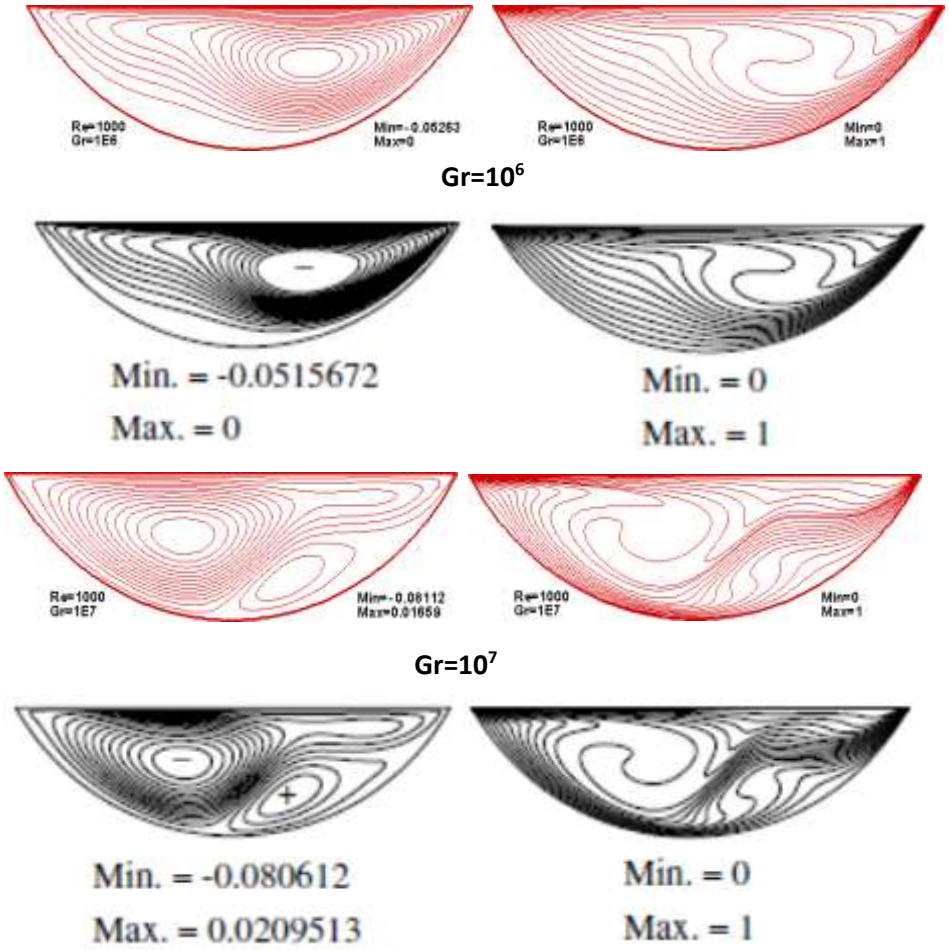

Figure 3. Validation study, Red (Present results) and Black [20] at Re=1000.

RESULTS AND DISCUSSION

Streamlines and isotherms

The effect of Richardson number (Ri=0.01, 0.1, 1, and 10) and inclination angle (φ =0º, 45º, and 90º) for three types (1, 2, and 3) of a wavy cavity on the behavior of fluid flow and thermal fields was studied at Gr=7142 as shown in Figure 4. These figures show that at low values of Ri number, The shear effect is dominant due to the rotation of the top wall. The fluid flow is driven by a main counter - current eddy of the cavity size which is formed by the top lid movement. The isothermal contour charts are grouped close to the low and high walls leading to a high gradient of temperature. At low Richardson number, the vorticity seems to be weak at the upper part of cavity. As Ri increases the natural convection starts to grew and create circulation to supports the upper vorticity which starts to creep towards the bottom wall of the cavity with increase Richardson number and the convection current becomes more dominant resulting in stronger flow field. The maps of isotherms change accordingly with streamlines, and as Ri number significantly increases the changes in the isotherm diagram, the dominant heat transfer for this particular case is indicating the natural convection. On the other hand, due to the dominance of the natural convection, the shear induced circulation at the upper wall side becomes smaller and smaller with Ri number increase.The effect of changing the cavity type (i.e., different amplitudes) show that the combined effect of primary and secondary flows increases with increment amplitude and number of corrugations; respectively. It is found that the isotherms are thinner in the region adjacent to the heated wall surface to

create higher temperature vectors, growing the amplitude. Also, the figure shows that the increasing of amplitude and number of corrugations (type 4) leads to enhance the heat transfer rates.

Type 1, $\varphi = 0^o$

	$\Psi = -0.002 \ \ to - 0.028$	$\theta = 0 \ \ to \ \ 1$
Ri =0.01		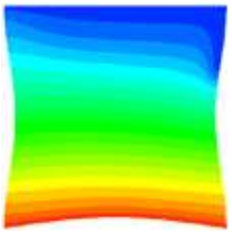
Ri =0.1	$\Psi = -0.005 \ \ to - 0.095$	$\theta = 0 \ \ to \ \ 1$
		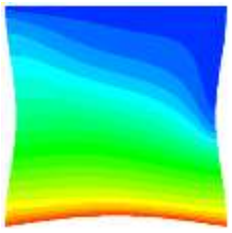
Ri =1	$\Psi = -0.01 \ \ to - 0.17$	$\theta = 0 \ \ to \ \ 1$
	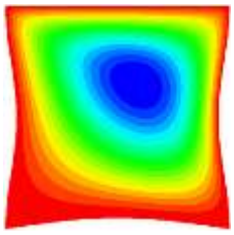	
Ri =10	$\Psi = -0.02 \ \ to - 0.028$	$\theta = 0 \ \ to \ \ 1$
	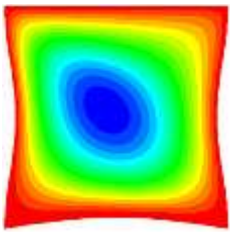	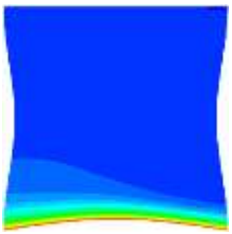

Type 2. $\varphi = 90^{o}$

Ri =0.01 $\Psi = -0.002 \;\; to \; -0.028$ $\theta = 0 \;\; to \;\; 1$

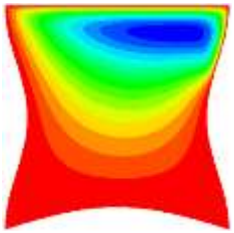

Ri =0.1 $\Psi = -0.005 \;\; to \; -0.095$ $\theta = 0 \;\; to \;\; 1$

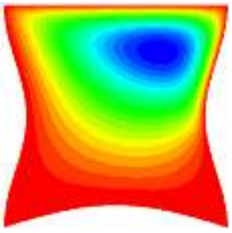

Ri =1 $\Psi = -0.01 \;\; to \; -0.17$ $\theta = 0 \;\; to \; 1$

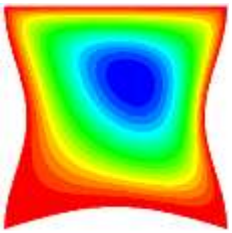

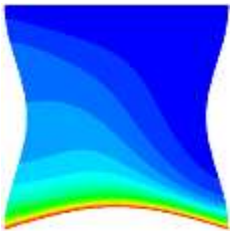

Ri =10 $\Psi = -0.02 \;\; to \; -0.34$ $\theta = 0 \;\; to \; 1$

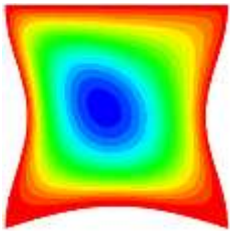

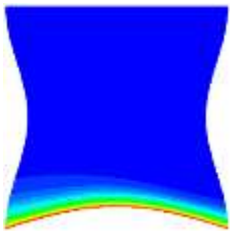

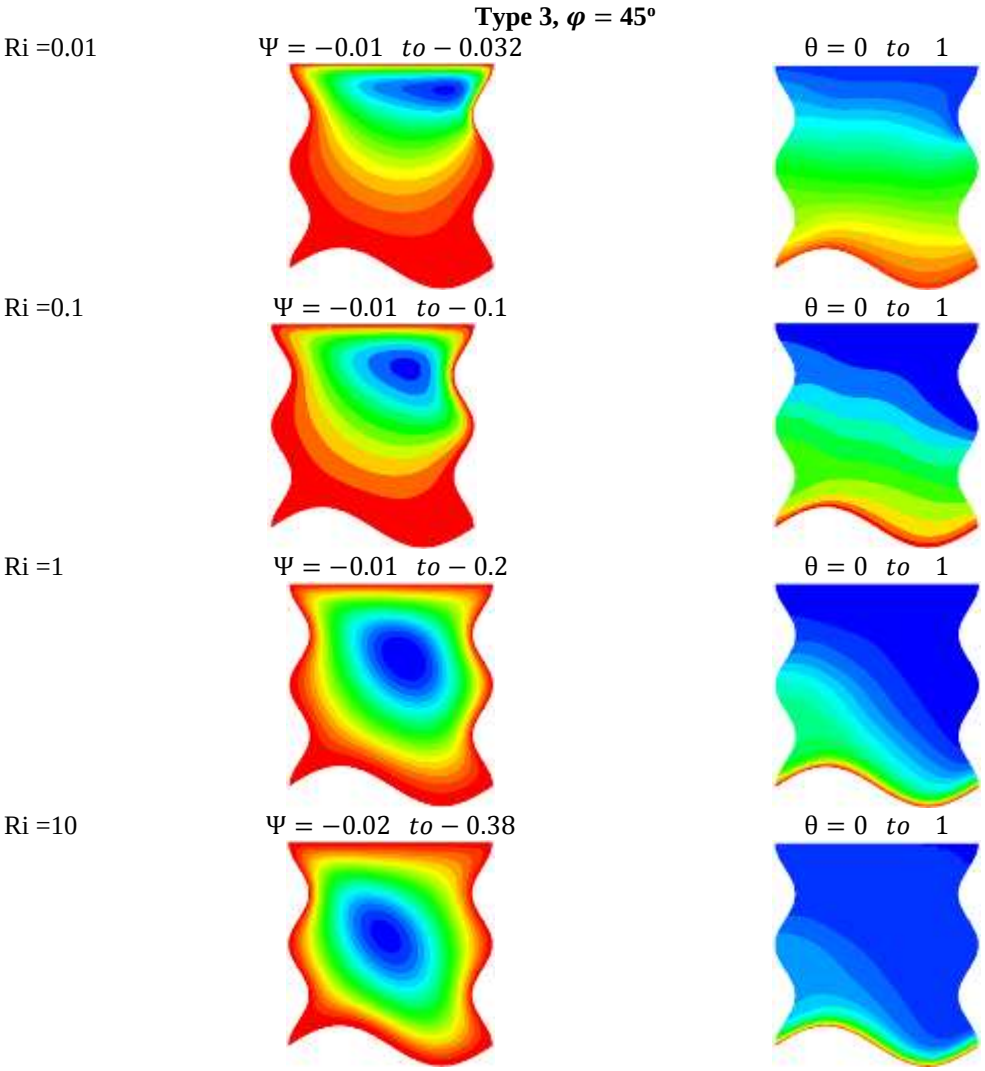

Figure 4: Streamlines and isotherms contour for three types of wavy cavity at three angles of inclination and different Richardson numbers.

Average Nusselt number

Figure 5 shows the variation of average Nusselt number with Richardson number for four types of wavy cavity at different angles of inclination. The results show that there is no effect for the angle of cavity inclination on the heat transfer process. The values of average Nusselt number increases as Richardson number increases. This effect could be due to the point that the nozzle-driven becomes more involved in through the transfer of heat. It was shown that type 4 of wavy cavity gives higher heat transfer rates than, type two, type 3, and type one; respectively.

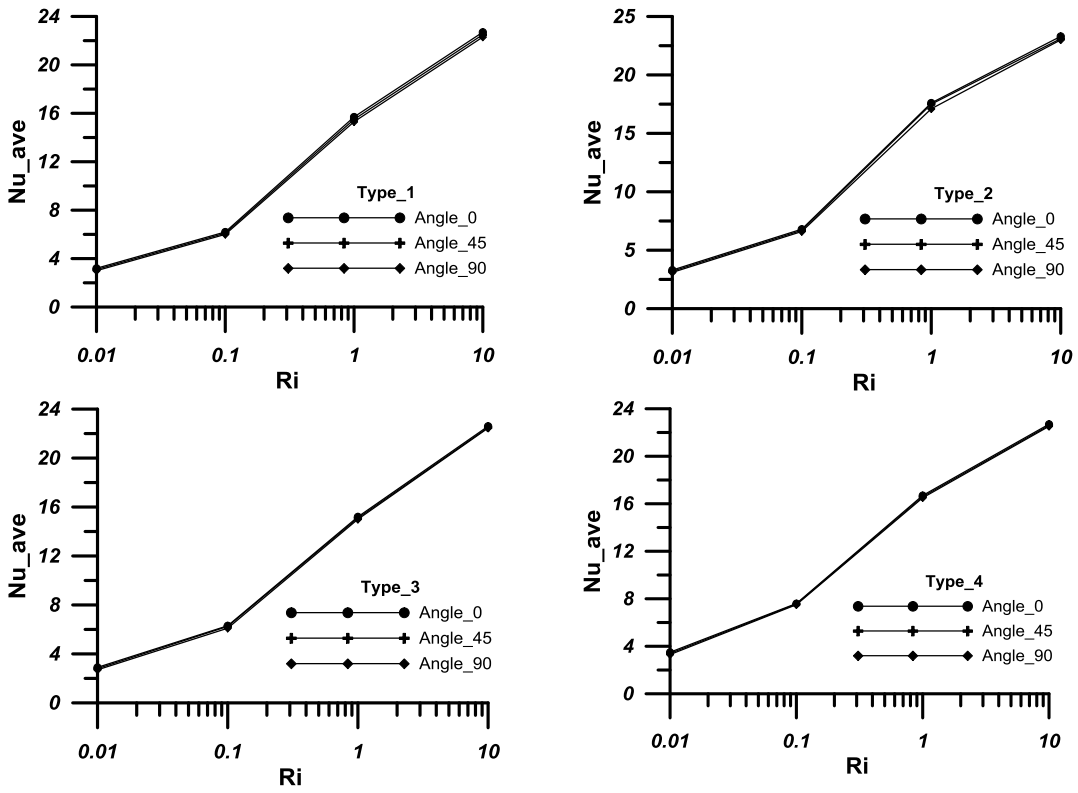

Figure 5. Average Nusselt number versus Richardson number for four types of wavy cavity at different angles of inclination

CONCLUSIONS

It was found that the thermal fields and the fluid flow characteristics inside wavy cavity with lid-driven are strongly dependent on the Richardson number.

The Nusselt number increases with Richardson number.

There is no result of angle of inclination on the heat transfer process inside cavity with lid-driven.

It was shown that type 4 of wavy cavity gives higher heat transfer rates than, type two, type 3, and type one; respectively.

The heat transfer coefficient enhances in a wavy cavity as the amplitude and number of corrugations increase.

NOMENCLATURE

c_1, c_2, c_3	coordinate transformation coefficients	u, v	velocity components in x- and y-directions, respectively
f_x	local friction factor		
g	gravitational acceleration	U, V	dimensionless velocity compon
Gr	Grashof number		x- and y-directions, respectivel
h	overall heat transfer coefficient	u_o	constant velocity of moving lid
h_x	local heat transfer coefficient	x, y	rectangular coordinates
J	Jacobian of coordinate transformation	X, Y	dimensionless rectangular coo
κ	thermal conductivity of fluid	α	fluid thermal diffusivity
N	number of corrugations	β	coefficient of volume expansio
Nu_{ave}	overall Nusselt number	λ	amplitude
Nu_x	local Nusselt number	φ	inclination angle
Pr	Prandtl number	μ	dynamic viscosity of fluid
Re	Reynolds number	ϑ	kinematic viscosity of fluid
Ri	Richardson number ($Ri = Gr/Re^2$)	ξ, η	body-fitted curvilinear coordina
T	fluid temperature	τ_x	local shear stress
θ	dimensionless temperature	ϕ	stream function
T_h	higher temperature at side walls	Ψ	dimensionless stream function
T_l	lower temperature at base wal	ω	vorticity
		Ω	dimensionless vorticity

REFERENCES

[1] C.L. Chen, C.H. Cheng, "Experimental and numerical study of mixed convection and flow pattern in a lid-driven arc-shape cavity", *Heat Mass Transfer*, vol. 41, pp. 58–66, 2004.

[2] H.F. Oztop, "Combined convection heat transfer in a porous lid-driven enclosure due to heater with finite length", *International Communications in Heat and Mass Transfer*, vol. 33, pp. 772–779, 2006.

[3] M. A. R. Sharif, "Laminar mixed convection in shallow inclined driven cavities with hot moving lid on top and cooled from bottom", *Applied Thermal Engineering*, 27, pp. 1036–1042, 2007.

[4] C. A. Chaves, J. R. Camargo, and V. A. Correa, "Combined forced and free convection heat transfer in a semiporous open cavity," Sci. Res. Essay, vol. 3m no. 8, pp. 333–337, 2008.

[5] C.Y. Wang, "The recirculating flow due to a moving lid on a cavity containing a Darcy–Brinkman medium", *Applied Mathematical Modeling*, vol. 33, pp. 2054–2061, 2009.

[6] S. Chung, K. Vafai, "Vibration induced mixed convection in an open-ended obstructed cavity" *International Journal of Heat and Mass Transfer*, vol. 53, pp. 2703–2714, 2010.

[7] M.A. Mohd Irwan, A. M. Fudhail, C.S. Nor Azwadi and G. Masoud, "Numerical Investigation of Incompressible Fluid Flow through Porous Media in a Lid-Driven Square Cavity", *American Journal of Applied Sciences*, vol. 7, no. 10, pp. 1341-1344, 2010.

[8] H. Nemati, M. Farhadi, K. Sedighi, E. Fattahi, A. A. R. Darzi, "Lattice Boltzmann simulation of nanofluid in lid-driven cavity", *International Communications in Heat and Mass Transfer*, vol. 37, pp. 1528–1534, 2010.

[9] M. M. Rahman, M. M. Billah, A. T. M. M. Rahman, M. A. Kalam, A. Ahsan, "Numerical investigation of heat transfer enhancement of nanofluids in an inclined lid-driven triangular enclosure", *International Communications in Heat and Mass Transfer*, vol. 38, no. 10, pp. 1360-1367, 2011.

[10] G.F. Al-Sumaily, A. Nakayama, J. Sheridan, M.C. Thompson, "The effect of porous media particle size on forced convection from a circular cylinder without assuming local thermal equilibrium between phases", *International Journal of Heat and Mass Transfer*, vol. 55, pp. 3366–3378, 2012.

[11] K. Al-Salem, H.F. Oztop, I. Pop, and Y. Varol, "Effects of moving lid direction on MHD mixed convection in a linearly heated cavity", *International Journal of Heat and Mass Transfer*, vol. 55, pp. 1103–1112, 2012.

[12] G.F. Al-Sumaily, M.C. Thompson, "Forced convection from a circular cylinder in pulsating flow with and without the presence of porous media", *International Journal of Heat and Mass Transfer*, vol. 61, pp. 226–244, 2013.

[13] A.M. Aly and S.E. Ahmed, "An incompressible smoothed particle hydrodynamics method for natural/mixed convection in a non-Darcy anisotropic porous medium", *International Journal of Heat and Mass Transfer*, vol. 77, pp. 1155-1168, 2014.

[14] C.L. Chen and Y.C. Chung, "Numerical Study on Mixed Convection Heat Transfer on Inclined Triangular Cavities", *Numerical Heat Transfer*, Part A, vol. 67, pp. 651–672, 2015.

[15] J. Burgos, I. Cuesta, C. Salueñ, "Numerical study of laminar mixed convection in a square open cavity", *International Journal of Heat and Mass Transfer*, vol. 99, pp. 599–612, 2016.

[16] I. Zeghbid and R. Bessaïh, "Mixed Convection in a Lid-Driven Square Cavity with Heat Sources Using Nanofluids", FDMP, vol. 13, no. 4, pp. 251-273, 2017.

[17] A.K. Kareem, H. A. Mohammed, A.K. Hussein, S. Gao, "Mixed convection heat transfer in a lid-driven trapezoidal enclosure filled with nanofluids".

[18] G.H.R. Kefayati, H. Tang, "MHD mixed convection of viscoplastic fluids in different aspect ratios of a lid-driven cavity using LBM", *International Journal of Heat and Mass Transfer*, vol. 124, pp. 344–367, 2018.

[19] J. F. Thompson, F. C. Thames, and C. W. Mastin, "Automatic Numerical Generation of Body-Fitted Curvilinear Coordinate System for Filed Containing Any Number of Arbitrary Two-Dimensional Bodies", *J. Comput. Phys.*, vol. 15, pp. 299–319, 1974.

[20] C. L. Chen and C. H. Cheng, Numerical Prediction of Buoyancy-Induced Periodic Flow Pattern and Heat Transfer in a Lid-Driven Arc-Shape Cavity", *Numer. Heat Transfer A. Appl.*, vol. 44, pp. 645–663, 2003.

[21] C. H. Cheng and C. L. Chen, Numerical Study of Effects of Inclination on Buoyancy-Induced Flow Oscillation in a Lid-Driven Arc-Shaped Cavity", Numer. *Heat Transfer A. Appl.*, vol. 48, pp. 77–97, 2005.

[22] C. L. Chen and C. H. Cheng, Periodic Flow Pattern and Convection Heat Transfer in an Arc-Shaped Cavity with Oscillating Lid, Numer. Heat Transfer". *A.-Appl.*, vol. 50, pp. 491–507, 2006.